

# Post-Accident Sporadic Releases of Airborne Radionuclides from the Fukushima Daiichi Nuclear Power Plant Site

Georg Steinhauser,<sup>†,‡,¶,¶</sup> Tamon Niiso,<sup>‡</sup> Kouji H. Harada,<sup>§</sup> Katsumi Shozugawa,<sup>||</sup> Stephanie Schneider,<sup>‡</sup> Hans-Arno Synal,<sup>#</sup> Clemens Walther,<sup>‡</sup> Marcus Christl,<sup>#</sup> Kenji Nanba,<sup>¶</sup> Hirohiko Ishikawa,<sup>‡</sup> and Akio Koizumi<sup>\*,§</sup>

<sup>†</sup>Colorado State University, Environmental and Radiological Health Sciences, Fort Collins, Colorado 80523, United States

<sup>‡</sup>Research Division of Atmospheric and Hydrospheric Disasters, Disaster Prevention Research Institute, Kyoto University, Uji 6110011, Japan

<sup>§</sup>Department of Health and Environmental Sciences, Kyoto University Graduate School of Medicine, Kyoto 6068501, Japan

<sup>||</sup>Graduate School of Arts and Sciences, The University of Tokyo, Meguro-ku, Tokyo 153-8902, Japan

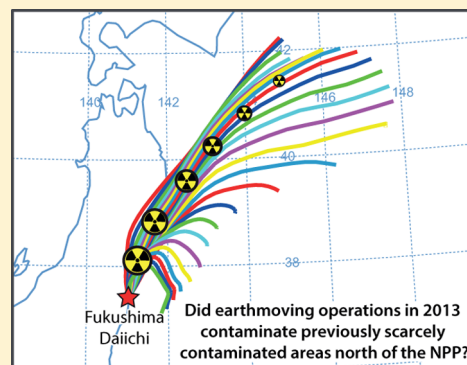
<sup>‡</sup>Leibniz Universität Hannover, Institute of Radioecology and Radiation Protection, D-30419 Hannover, Germany

<sup>#</sup>Laboratory of Ion Beam Physics, ETH Zürich, CH-8093 Zürich, Switzerland

<sup>¶</sup>Institute of Environmental Radioactivity, Fukushima University, Fukushima 960-1296, Japan

## Supporting Information

**ABSTRACT:** The Fukushima nuclear accident (March 11, 2011) caused the widespread contamination of Japan by direct deposition of airborne radionuclides. Analysis of weekly air filters has revealed sporadic releases of radionuclides long after the Fukushima Daiichi reactors were stabilized. One major discharge was observed in August 2013 in monitoring stations north of the Fukushima Daiichi nuclear power plant (FDNPP). During this event, an air monitoring station in this previously scarcely contaminated area suddenly reported  $^{137}\text{Cs}$  activity levels that were 30-fold above the background. Together with atmospheric dispersion and deposition simulation, radionuclide analysis in soil indicated that debris removal operations conducted on the FDNPP site on August 19, 2013 are likely to be responsible for this late release of radionuclides. One soil sample in the center of the simulated plume exhibited a high  $^{90}\text{Sr}$  contamination ( $78 \pm 8 \text{ Bq kg}^{-1}$ ) as well as a high  $^{90}\text{Sr}/^{137}\text{Cs}$  ratio (0.04); both phenomena have usually been observed only in very close vicinity around the FDNPP. We estimate that through the resuspension of highly contaminated particles in the course of these earthmoving operations, gross  $^{137}\text{Cs}$  activity of ca.  $2.8 \times 10^{11} \text{ Bq}$  has been released.



## INTRODUCTION

Radionuclides released in the course of the Fukushima nuclear accident (March 11, 2011) have caused severe contamination of parts of the Japanese mainland.<sup>1,2</sup> The damaged reactors of the Fukushima Daiichi nuclear power plant (FDNPP) released mainly radionuclides of volatile elements, such as  $^{131}\text{I}$ ,  $^{132}\text{Te}$ ,  $^{134}\text{Cs}$ ,  $^{136}\text{Cs}$ , and  $^{137}\text{Cs}$ ,<sup>3,4</sup> of which only radiocesium nuclides  $^{134}\text{Cs}$  ( $T_{1/2} = 2.07 \text{ y}$ ) and  $^{137}\text{Cs}$  ( $T_{1/2} = 30.08 \text{ y}$ ) are sufficiently long-lived to cause a long-term contamination of the affected areas. The largest amounts of radiocesium were deposited in a  $3000 \text{ km}^2$  area northwest of the FDNPP.<sup>5</sup>

Although located at a very close range to this NW-contamination strip, only minor amounts of radiocesium were deposited in the areas north of FDNPP.<sup>6</sup> However, two unusual detections of  $^{90}\text{Sr}$  ( $T_{1/2} = 28.8 \text{ y}$ ) and Pu with a “reactor signature” were made in vegetation samples from Minamisoma (taken in December 2011, approximately 16 km north of FDNPP)<sup>7,8</sup> that challenged the expectations of a very low

degree of contamination. Generally, radionuclides with medium ( $^{90}\text{Sr}$ ) or low volatility ( $^{239,240}\text{Pu}$ ) have been emitted from the FDNPP in low but detectable amounts.<sup>9–11</sup> These findings of environmental samples with an unusually high  $^{90}\text{Sr}/^{137}\text{Cs}$  activity ratio<sup>7</sup> and a high  $^{240}\text{Pu}/^{239}\text{Pu}$  isotopic ratio<sup>8</sup> from locations relatively far from the FDNPP, however, did not fit into the expected distribution pattern and raised the question of the existence of a different source or release mechanism which may be responsible for these unusual findings of refractory radionuclides in a low-contaminated area. In the present study, we investigated the hypothesis that resuspension of highly contaminated particles from the FDNPP site may be responsible for the observed anomalies and the late

Received: June 30, 2015

Revised: October 6, 2015

Accepted: October 8, 2015

Published: October 8, 2015

contamination of the previously little affected area north of FDNPP. The primary focus of this study is the debris removal operations from the FDNPP site on August 19, 2013.

## MATERIALS AND METHODS

**Air Filter Radioanalysis.** Air filters were installed in October 2012 in three locations north (Haramachi/Minamisoma), northwest (Tamano/Soma), and southwest of the FDNPP (Kamikawauchi/Kawauchi) and analyzed weekly for radioactive particles. The entire airborne dust in the air was collected weekly on quartz membrane filters using a high-volume sampler at flow rates of 500–1000 L/min (HV-1000F, Sibata, Saitama, Japan). Aerodynamic diameter-fractionated dust samples (100–11.4  $\mu\text{m}$  to  $<0.46 \mu\text{m}$ ) were collected using an Andersen cascade impactor sampler (AN-200, Tokyo Dylec Co., Tokyo, Japan) at a flow rate of 28.2 L/min. Unless otherwise stated, all activities were decay corrected to the time of sampling.

**Soil Sampling.** Twenty-one soil samples were taken on September 7, 2014 in the Minamisoma area (Figure S1) and investigated for  $\gamma$ -emitting radionuclides ( $^{134}\text{Cs}$ ,  $^{137}\text{Cs}$ ), as well as for  $^{90}\text{Sr}$  and Pu. Dose rates on each location were measured in 1 m above ground (see Table S1). After removal of surface vegetation (excluding roots), sampling was performed with a drill core auger that yielded drill cores inside of plastic sleeves of 15 cm length and an inner diameter of 4.7 cm. In the laboratory, the sleeves were cut into six disk-shaped segments of 2.5 cm thickness each.

**Radiocesium Analysis.** Radiocesium activity concentrations in air filters and soil sample disks were analyzed by HPGe  $\gamma$ -spectrometry (Ortec GEM-15190). Dust sampling filters were packed in thin polyethylene containers (8 cm i.d., 0.5 cm height). Soil samples were filled in polyethylene cylinders (U8 container). Measurement durations were  $>40\,000$  s for air filter samples and  $>10\,000$  s for soil samples. Cesium-134 and -137 were quantified by their 604.7 and 661.7 keV photons, respectively. Peak summing effects of  $^{134}\text{Cs}$  were corrected.

**Soil Radiostrontium Analysis.** Analyzing only the top layer (2.5 cm) of each soil drill core was deemed sufficient for the purpose of this study, as previous analyses of drill cores from the area have shown that—if any—only the top layer exhibited  $^{90}\text{Sr}$  levels that are clearly elevated above background. Plutonium is characterized by a generally low mobility in the environment, as Mahara and Miyahara found migration rates of  $1.25 \text{ mm y}^{-1}$  for Pu from Nagasaki.<sup>12</sup> After drying the entire sample at  $100^\circ\text{C}$  for 24 h, approximately one-quarter of each disk was used (approximately 6 to 10 g) for analysis. For radiostrontium analysis using liquid scintillation counting (LSC), the separation of the Sr fraction is imperative. The procedure was conducted according to our previously developed analytical protocol.<sup>7</sup> Here, the procedure was conducted in two steps, the first of which was done at Fukushima University, and the second at Colorado State University. In brief, at Fukushima University, the samples were leached with a mixture of 4 mL  $\text{HNO}_3$  (8 M), 1 mL concentrated  $\text{H}_2\text{O}_2$  (30%), 1 mL of aqueous stable Sr carrier ( $c_{\text{Sr}} = 1.2 \text{ mg}\cdot\text{mL}^{-1}$  in  $\text{H}_2\text{O}$ ), and 2 mL of concentrated  $\text{HNO}_3$  (70%). The mixture was boiled for 30–40 min under reflux and filtered through a paper filter. The filter cake was rinsed with approximately 10 mL of 8 M  $\text{HNO}_3$ . The filtrate was loaded onto Eichrom's SR resin (2 mL cartridge), washed with 6 mL 8 M  $\text{HNO}_3$ . Then the cartridges were sealed and transferred to Colorado State University. There the resin was washed with a

total 30 mL of 8 M  $\text{HNO}_3$  and rinsed with  $5 \times 1 \text{ mL}$  of an aqueous solution of 3 M  $\text{HNO}_3 + 0.05 \text{ M}$  oxalic acid. In this washing/rinsing procedure, foreign radionuclides such as  $^{134+137}\text{Cs}$  and  $^{90}\text{Y}$  (the daughter of  $^{90}\text{Sr}$ ) were removed quantitatively. The Sr fraction was then eluted using  $10 \times 1 \text{ mL}$  of 0.01 M  $\text{HNO}_3$ , which has proven to retain any interfering  $^{210}\text{Pb}$  on the column, but to elute  $^{90}\text{Sr}$  efficiently.<sup>13</sup> This elution procedure was done very slowly to allow the  $\text{Sr}^{2+}$  ions to migrate out of the pores. We also followed the recommendation of Eichrom and introduced a break of at least 1 h after the first 5 mL of elution. The eluate was steamed off to almost dryness and then taken up in 1 mL of autoclaved and deionized  $\text{H}_2\text{O}$ . This step was repeated 10 times and most of the acid removed to allow for perfect mixing with the Ultima Gold scintillation cocktail. The remaining liquid was transferred into LSC vials and mixed with 18 mL scintillation cocktail. After the separation, the LSC vials were measured for 6000 s with a HIDEX 300 SL scintillation counter (4 replicates, the first of which was discarded due to possible fluorescence effects in the cocktail after exposure to light). After ingrowth of  $^{90}\text{Y}$  (at least 16 days after the first measurement), a second measurement was done, analyzing the sum activities of  $^{90}\text{Sr} + ^{90}\text{Y}$ . This measurement was used also for quality control purposes, as it allows checking if the count rate almost doubled due to the ingrowth of the  $^{90}\text{Y}$ . Sample vials with LSC-detectable activities were also measured on an HPGe  $\gamma$ -detector to check for any residual  $^{134+137}\text{Cs}$  activities (however, no traces of any interfering radiocesium could be detected).

The extraction efficiency (Sr yield) of this procedure was 85% from soil, as determined using  $\gamma$ -emitting  $^{85}\text{Sr}$ . For quantification, we used the reference material IAEA-373 (Radionuclides in Grass), which has a certified  $^{90}\text{Sr}$  activity concentration. We applied the same extraction procedure to the reference material and found an extraction yield of 85% using an IAEA-373 aliquot spiked with  $^{85}\text{Sr}$ .

**Soil Plutonium Analysis.** Another quarter of the top surface soil disks (approximately 6–10 g) was used for plutonium extraction and analysis. The dried soil aliquot was weighed and ashed at  $450^\circ\text{C}$  for at least 2 h to remove organics. Then,  $1.52 \pm 0.03 \text{ mBq}$  or  $(2.58 \pm 0.06) \times 10^{10}$  atoms of a  $^{242}\text{Pu}$  tracer were added (50  $\mu\text{L}$  of a solution with  $c_{\text{Pu-242}} = 0.0304 \pm 0.000654 \text{ Bq/mL}$ ) prior to leaching with 7 mL aqua regia and refluxing for 30 min. Bisinger et al.<sup>14</sup> found that leaching of Pu with aqua regia works well for geological sample matrices with high silica content. After leaching, the insoluble residue was filtered off using a paper filter. The filtrate was evaporated to dryness. The solid residue was taken up in concentrated  $\text{HNO}_3$  and evaporated again. The residue was taken up in an aqueous solution of 3 M  $\text{HNO}_3$  and 1 M  $\text{Al}(\text{NO}_3)_3$ . In order to fix the valency of the analyte to  $\text{Pu}^{\text{IV}}$ , the mixture was first reduced with 750  $\mu\text{L}$  of a 40.8%  $\text{Fe}^{\text{II}}$  sulfamate solution. After waiting for 5 min, 500  $\mu\text{L}$  of an aqueous 3.5 M  $\text{NaNO}_2$  solution were added (Caution! This step may cause the vigorous emission of poisonous  $\text{NO}_x$  gas!). The sample solution was filled up to 35 mL using 3 M  $\text{HNO}_3$  before loading on preconditioned Eichrom TEVA resin columns (2 mL) and rinsing with 3 M  $\text{HNO}_3$ . The columns were transferred to Leibniz Universität Hannover for the final purification and workup. There, as the first step, the Pu was eluted using 0.1% hydroxylamine solution. Then the eluate was evaporated on a hot plate and then redissolved with 3 M  $\text{HNO}_3$ . A second separation step was applied to optimize the separation between U and Pu using the TEVA resin. The Pu

was coprecipitated together with  $\text{Fe}(\text{OH})_3$ . To remove any interfering compounds, a centrifuge step was implemented and the residue was washed with methanol. Afterward the residue was transferred into porcelain crucibles. By heating up to  $800^\circ\text{C}$  the  $\text{Fe}(\text{OH})_3$  was calcined to form  $\text{Fe}_2\text{O}_3$ . Finally the sample was mixed with metallic Nb powder in a ratio of 1:1 and pressed into an AMS target holder.

The accelerator mass spectrometry (AMS) measurement of Pu isotopes was performed at the Laboratory of Ion Beam Physics of ETH Zurich, Switzerland, using the upgraded compact, low energy AMS facility “Tandy”.<sup>15</sup> With a transmission of up to 40% for uranium and thorium,<sup>16</sup> an abundance sensitivity on the order of  $10^{-12}$ ,<sup>17</sup> and detection limits in the subfemtogram range for Pu isotopes,<sup>18</sup> the compact (lab-sized) ETH Zurich AMS system Tandy is well suited to detect ultratrace amounts of actinides.<sup>8</sup>

Details of the AMS measurement of Pu samples are described in ref 8. In this study, the  $^{239,240,242}\text{Pu}$ -isotopes were measured sequentially for 15, 25, and 8 s, respectively. A possible interference of  $^{238}\text{U}$  ions with  $^{239}\text{Pu}$  was (caused by “tailing” of  $^{238}\text{U}$ ) was carefully monitored and turned out to be negligible for all samples. The isotopic ratios of interest were calculated from the repeated sequential measurement of samples and standards. Each sample was measured for about 35 min in total.

The measured Pu ratios were normalized to the ETH in-house standard “CNA”<sup>19</sup> and corrected for impurities ( $^{239}\text{Pu}$  and  $^{240}\text{Pu}$ ) carried by the  $^{242}\text{Pu}$  spike material. The uncertainty of the reported ratios includes counting statistics, the variability of the measured isotopic ratios of both samples and standards, and the uncertainty of the spike correction. The uncertainty of the  $^{239,240}\text{Pu}$  concentrations additionally includes the uncertainty of the spike  $c_{242}$ .

### Atmospheric Dispersion and Deposition Simulation.

We simulated atmospheric dispersion and deposition of  $^{137}\text{Cs}$  emitted from the FDNPP on August 19, 2013 during debris removal operations using version 3.6.1 of the fully coupled Weather Research and Forecasting/Chemistry (WRF-Chem) model.<sup>20,21</sup> In WRF-Chem, dispersion and deposition of constituents in the atmosphere are consistent with the meteorological fields simultaneously calculated by the non-hydrostatic WRF framework. We have two computational domains including the FDNPP (Figure 1). Domain 1 was 500 km wide from west to east and 600 km wide from south to north. Domain 2 was 90 km wide square. The horizontal

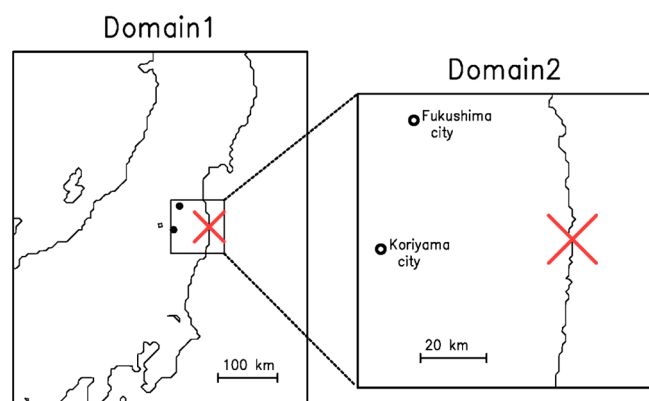


**Figure 1.** Computational domains. The red cross indicates the location of FDNPP.

resolutions for Domain 1 and 2 were 5 km and 1 km, respectively. The two domains communicated with each other through two-way nested runs; Domain 1 provided the boundary conditions to Domain 2, which fed computational results back to the mother domain. Both domains had the same vertical structure of 40 layers from the surface to 50 hPa with a pressure-based terrain-following coordinate system. The typical depth of the lowest layer was about 70 m. The initial conditions of both domains and boundary ones of Domain 1 for meteorological prediction were derived from 3-hly analyses with the mesoscale model of the Japan Meteorological Agency.<sup>22</sup>

Cesium-137 is transported by grid-resolved wind fields and subgrid scale mixing, and removed by wet and dry deposition as particulate matter. Gravitational settling was considered in the transport and dry deposition processes. We observed a size distribution of  $^{137}\text{Cs}$  bound to atmospheric dust with an activity weighted average on a logarithmic scale of  $4.8\ \mu\text{m}$  in Minamisoma City in August 2013 (Figure 2), and used a fixed diameter of  $4.8\ \mu\text{m}$  for  $^{137}\text{Cs}$  in the model. Effects of the particle diameter on the results were explored through sensitivity tests.

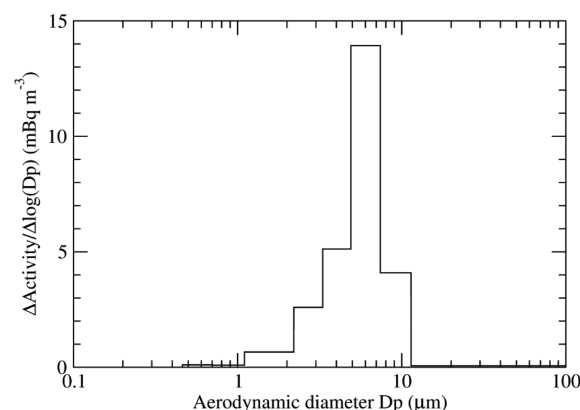


**Figure 2.** Size distribution of  $^{137}\text{Cs}$  bound to atmospheric dust observed in Minamisoma City in a period from first August to fifth September 2013. The activity weighted average on a logarithmic scale was  $4.8\ \mu\text{m}$ .

Nuclear Regulation Authority (NRA) estimated radioactivity emitted from the FDNPP site in the course of the debris removal operations on August 19, 2013 to be  $1.1 \times 10^{11}\ \text{Bq}$ ,<sup>23</sup> from which we derived the source term of  $^{137}\text{Cs}$  assuming emitted radionuclides were only  $^{134}\text{Cs}$  and  $^{137}\text{Cs}$ . We also assumed that any other emission was negligible. The total emission of  $^{137}\text{Cs}$  was  $7.7 \times 10^{10}\ \text{Bq}$  (Figure 3). Cesium-137 was emitted exclusively in the lowest layer at the grid cell corresponding to the FDNPP, because the emission height was estimated to be about 40 m by NRA.<sup>23</sup> The simulation period was 06:00 on August 19th to 09:00 on August 20th, 2013 (JST). An initial atmospheric  $^{137}\text{Cs}$  concentration of zero was assumed.

## RESULTS AND DISCUSSION

**Air Filter Radioanalysis.** In the course of this survey, several sporadic releases were observed months after the accident. We have checked press releases from the FDNPP operator (Tokyo Electric Power Company, TEPCO) and found that workers were reported to have been exposed to



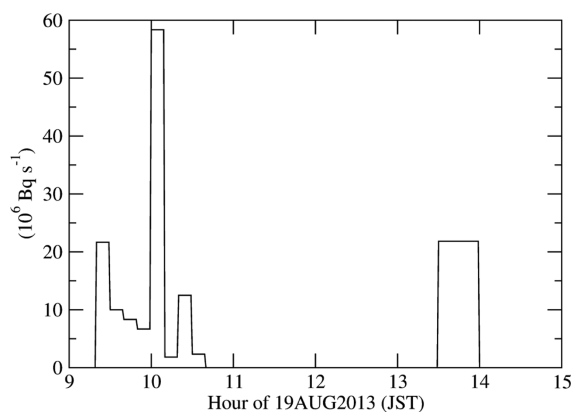


**Figure 3.** Cesium-137 emissions on August 19, 2013 used in the model ( $10^6 \text{ Bq s}^{-1}$ ). The emission values were derived from radioactivity estimated by NRA<sup>23</sup> assuming emitted radionuclides were only  $^{134}\text{Cs}$  and  $^{137}\text{Cs}$ . The total emission of  $^{137}\text{Cs}$  was  $7.7 \times 10^{10} \text{ Bq}$ .

relatively large amounts of radioactive dust in the same weeks when high activity concentrations in air were detected by the air filter stations. Resuspension of radiocesium bearing particles has been addressed previously as a potential source for the dispersion of radionuclides from the Fukushima nuclear accident.<sup>24,25</sup> Therefore, the hypothesis of this study has been that the radioactive particles observed in the air monitoring campaign originated from the FDNPP site. The most prominent event was observed on August 19, 2013 (Figure 4) in Minamisoma. Typical background values in these filter

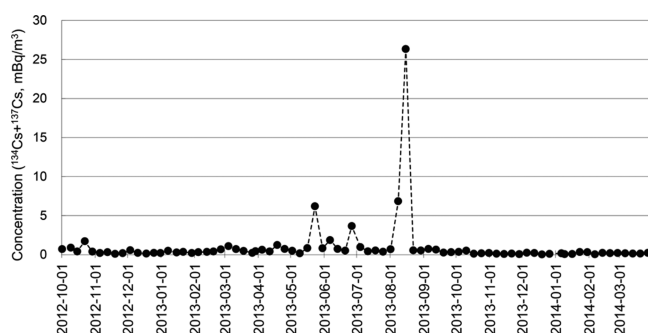


**Figure 4.** Radiocesium concentration in whole dust samples collected in Minamisoma City ( $37^{\circ}38'37'' \text{ N } 140^{\circ}55'27'' \text{ E}$ ) during October 1, 2012 to March 31, 2014. Dust samples were continuously collected on quartz fiber filters for ca. 7 days. Concentration shows the sum of  $^{134}\text{Cs}$  and  $^{137}\text{Cs}$  ( $\text{mBq m}^{-3}$ ) and is decay corrected to the date of sampling.

stations ranged from 0.04 to  $0.95 \text{ mBq m}^{-3}$ ; on August 19, 2013; however,  $26.3 \text{ mBq m}^{-3}$  have been measured. Prior to the Fukushima nuclear accident,  $^{137}\text{Cs}$  concentrations were in the range of  $\mu\text{Bq m}^{-3}$  or less, mainly due to the fallout of atmospheric nuclear explosions.

#### Atmospheric Dispersion and Deposition Simulation.

The model results showed that  $^{137}\text{Cs}$  emitted at the FDNPP on August 19, 2013 was dispersed toward our dust monitoring site located at Haramachi and Tamano (Figure 5). The dispersion pattern of the simulated  $^{137}\text{Cs}$  concentration in surface air was consistent with the observation that the radiation burst was recorded at Haramachi and Tamano but not at Kamikawauchi. The modeled concentrations were linear to the emission because radiocesium does not undergo chemical changes in the

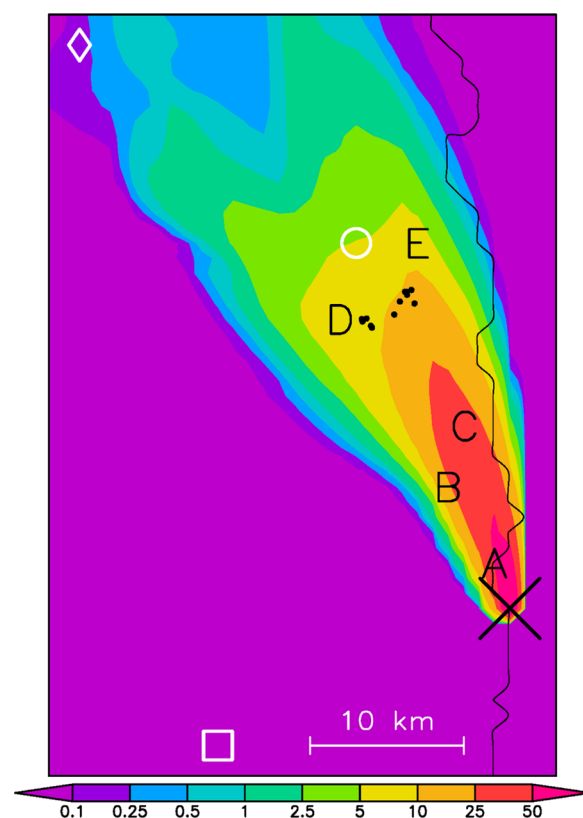


**Figure 5.** Distribution of  $^{137}\text{Cs}$  concentration ( $\text{mBq m}^{-3}$ ) in the surface air averaged for the period when the radiation burst incident was observed: August 5 to 22, 2013. We considered the emission from the FDNPP involved in the debris removal operations on August 19 only. The black  $\times$  indicates the FDNPP. The three white marks indicate dust monitoring sites Haramachi (O), Tamano ( $\diamond$ ), and Kamikawauchi ( $\square$ ), respectively. Black dots indicate soil sampling sites in the present study. The five characters, A–E, indicate locations of monthly deposition monitoring operated by Fukushima prefecture.<sup>26</sup>

atmosphere. Comparison with observations showed that the model underestimates concentrations based on the NRA report<sup>23</sup> by a factor of 3.61 at Haramachi and 4.35 at Tamano (Table 1), suggesting that the estimated magnitude of the emission on August 19, 2013 must have been greater at least by a factor of 3.61 (i.e.,  $3.61 \times 7.7 \times 10^{10} = 2.8 \times 10^{11} \text{ Bq}$ ). Since we considered only emissions involved in the debris removal operations at the FDNPP site in the period of 9:20 to 10:40 and 13:30 to 14:00 (JST) of this day as the source term (Figure 3), the modeled  $^{137}\text{Cs}$  concentrations in surface air outside of the downwind regions were as extremely low as shown at Kamikawauchi (Table 1). We had collected 51 samples of atmospheric dust at Kamikawauchi for about 1 week each in 2013, and found the minimum concentration of  $^{137}\text{Cs}$  to be  $0.015 \text{ mBq m}^{-3}$ , which could be interpreted as background level at Kamikawauchi. The underestimate by orders of magnitude at Kamikawauchi suggested that  $^{137}\text{Cs}$  observed at Kamikawauchi was caused by sources excluded in the model, emission at the FDNPP in another period than August 19, 2013, or resuspension from historical deposition.

We compared the monthly deposition of  $^{137}\text{Cs}$  in August 2013 between modeled values multiplied by a scale factor of 3.61 and observations at five monitoring sites operated by Fukushima prefecture on the direction of the dispersion from the FDNPP on August 19, 2013 in Futaba Town, Namie Town,

**Table 1. Comparison of Observed and Modeled  $^{137}\text{Cs}$  Concentrations ( $\text{mBq m}^{-3}$ ) in the Surface Air Averaged for the Period When the Radiation Burst Incident Was Observed, August 15 to 22, 2013**

site	city	<sup>a</sup>	distance from FDNPP (km)	<sup>137</sup> Cs concentration ( $\text{mBq m}^{-3}$ )	
				observed	modeled <sup>c</sup>
Haramachi	Minamisoma	○	26.2	18.4	5.09 (3.61)
Tamano	Soma	◇	47.7	0.883	0.203 (4.35)
Kamikawauchi	Kawauchi	□	21.8	0.181 <sup>b</sup>	7.48e−5 (2420)

<sup>a</sup>Geographical location in Figure 5. <sup>b</sup>Sample collected from August 9 to 20, 2013. <sup>c</sup>Factor of underestimate in parentheses.

**Table 2. Comparison of Monthly  $^{137}\text{Cs}$  Deposition ( $\text{Bq m}^{-2}$ ) on August 2013 between Observations Reported by Fukushima Prefecture<sup>26</sup> and Modeled Values Multiplied by a Scale Factor of 3.61**

site	city	<sup>a</sup>	latitude	longitude	distance from FDNPP (km)	<sup>137</sup> Cs monthly deposition ( $\text{Bq m}^{-2}$ )	
						observed	modeled <sup>b</sup>
Koriyama	Futaba	A	37.448	141.024	3.0	24000	702 (0.029)
Namie	Namie	B	37.494	140.991	8.9	420	362 (0.86)
Fukuura	Minamisoma	C	37.535	141.007	12.8	760	570 (0.75)
Baba	Minamisoma	D	37.599	140.907	22.7	81	112 (1.4)
Haramachi	Minamisoma	E	37.640	140.973	24.8	190	116 (0.61)

<sup>a</sup>Geographical location in Figure 5. <sup>b</sup>Multiplied by a scale factor of 3.61. Fractional portion to observed value in parentheses.

**Table 3. Sensitivity of Model Results to Particle Diameter<sup>a</sup>**

Site	<i>b</i>	distance from the FDNPP (km)	observed	modeled <sup>c</sup>		
				control (D <sub>p</sub> = 4.8 μm)	slow deposition case (D <sub>p</sub> = 2.5 μm)	fast deposition case (D <sub>p</sub> = 50 μm)
<sup>137</sup> Cs concentration (mBq m <sup>-3</sup> )						
Haramachi	○	26.2	18.4	18.4	20.8	6.99 × 10 <sup>-6</sup>
Tamano	◇	47.7	0.883	0.735	0.845	2.21 × 10 <sup>-9</sup>
<sup>137</sup> Cs monthly deposition (Bq m <sup>-2</sup> )						
Koriyama	A	3.0	24000	702	262	8510
Namie	B	8.9	420	362	177	27
Fukuura	C	12.8	760	570	282	16
Baba	D	22.7	81	112	59	0.003
Haramachi	E	24.8	190	116	61	0.01

<sup>a</sup>The modeled values were multiplied by a scale factor of 3.61. <sup>b</sup>Geographical location in Figure 5. <sup>c</sup>Multiplied by a scale factor of 3.61.

and Minamisoma City (Table 2). The simulated deposition fluxes can reproduce the observed ones at factors of 0.61–1.4 except Koriyama, a district in Futaba Town 3.0 km away from the FDNPP.

We conducted sensitivity tests to the particle diameter (Dp) (Table 3). Model results were fairly sensitive to Dp because there was no rainfall in the direction of the dispersion on August 19, 2013 so that gravitational settling was controlled mainly by Dp. By using Dp of 2.5  $\mu\text{m}$  (Slow Deposition Case), atmospheric concentrations increased moderately, while deposition fluxes decreased to about half of those by the control run. This made a negative demonstration for the possibility that the underestimation in the control run is due to excess gravitational settling (Table 1). Using Dp of 50  $\mu\text{m}$  (Fast Deposition Case), deposition flux at Koriyama increased by 1 order of magnitude, while those at Namie and Fukuura decreased by 1 order of magnitude, and a rather small amount of  $^{137}\text{Cs}$  was transported further than 20 km from the FDNPP. The results of the Fast Deposition Case suggested that the emission event on August 19, 2013 contained a large amount of radionuclides bound to coarse particles with a much greater diameter 4.8  $\mu\text{m}$  used in the control run, which was determined on the basis of the observation at Haramachi 26.2 km away from the FDNPP. It was also suggested that the monthly deposition of 24 000  $\text{Bq/m}^2/\text{month}$  observed at Koriyama was

due to mainly coarse particles, which were likely transported only to the closer vicinity of the FDNPP and not to the presently inhabited regions in the Minamisoma area.

It should be noted that the emitted particles had various sizes as observed in Haramachi (Figure 2), although we used a fixed Dp of 4.8  $\mu\text{m}$  in the control run. Particles with greater diameter (>1  $\mu\text{m}$ ) have faster deposition rates as demonstrated in the sensitivity tests so that using a greater Dp could increase the estimated value of the scale factor. However, it was also observed that particles with a diameter between 3.3 and 7.4  $\mu\text{m}$  contributed 68.6% to the total radioactivity. We confirmed that the modeled surface air concentration of  $^{137}\text{Cs}$  at Haramachi changed by only 38.1% using Dp of 3.3 or 7.4  $\mu\text{m}$ . Given theoretical rationality, we fully understand that the assumption on the particle size is critically sensitive for dry deposition. However, sensitivity analysis demonstrated that our results were robust even with uncertainties in particulate sizes.

**Soil Radioanalysis.** Soil samples from 21 sites in the Minamisoma area (Figure S1) were analyzed for  $^{134}\text{Cs}$ ,  $^{137}\text{Cs}$ ,  $^{239}\text{Pu}$ ,  $^{240}\text{Pu}$ , and  $^{90}\text{Sr}$ . Results for radiocesium are summarized in Table S1. Cesium-137 deposition (down to 15 cm depth) revealed a very ununiform picture with great local fluctuations (Figure S2). Figure S2 reveals that the radiocesium deposition

exhibits great differences even between locations in a short distance.

We also attempted the identification of the respective source of a contamination by  $^{134}\text{Cs}/^{137}\text{Cs}$  activity ratios. This method can reveal different sources, because  $^{134}\text{Cs}$  buildup in nuclear fuel is a function of fuel burn-up.<sup>27,28</sup> We found that the  $^{134}\text{Cs}/^{137}\text{Cs}$  ratios were roughly consistent in the top three layers of the soil cores (Figures S3a and S3b). Hence the average of the top three layers (7.5 cm) was used to calculate the  $^{134}\text{Cs}/^{137}\text{Cs}$  ratio of each spot as of the day of sampling (September 7, 2014) (Figure 6).

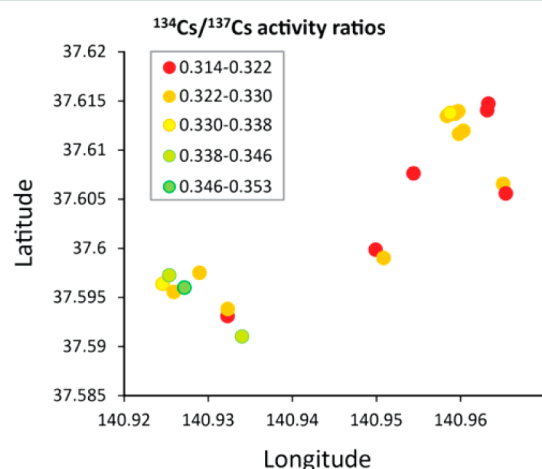


**Figure 6.** Radiocesium ratios in the top 7.5 cm of soil in the Minamisoma area (decay-corrected to the date of sampling on September 7, 2014).

The majority of the eastern locations seem to be contaminated with radiocesium with a lower  $^{134}\text{Cs}/^{137}\text{Cs}$  ratio, whereas the western locations tend to higher  $^{134}\text{Cs}/^{137}\text{Cs}$  activity ratios (with one exception: sample 9–1), which indicates that probably different sources have contaminated these very close locations. The activity ratio data in Table S1 show that these differences are at least partly statistically significant. A current press release from TEPCO indicates that reactor unit 3 of FDNPP could be the source of the contaminations owing to its characteristic low  $^{134}\text{Cs}/^{137}\text{Cs}$  activity ratio.<sup>29</sup> Air samples taken by TEPCO in close vicinity to unit 3 show a low  $^{134}\text{Cs}/^{137}\text{Cs}$  activity ratio of 0.28 (decay corrected to the day of sampling on September 7, 2014). It is interesting, however, that the activity in the air filter from Haramachi/Minamisoma reveals a high  $^{134}\text{Cs}/^{137}\text{Cs}$  activity ratio of 0.375 (decay corrected to September 7, 2014) (Table S2).

The presence of refractory radionuclides may be a much more conclusive indicator for contaminations of the Minamisoma area with airborne dust from the FDNPP site. As shown in previous studies, both  $^{90}\text{Sr}$ <sup>7</sup> as well as Pu<sup>8</sup> activity concentrations were significantly higher next to the FDNPP site. Material dispersed from the site hence is expected to carry a relatively high fraction of low-volatile radionuclides such as  $^{90}\text{Sr}$  or reactor Pu.

Environmental samples, especially soil, often contain detectable traces of Pu as a result of the fallout from the atmospheric nuclear explosions of the 20th century. Reactor plutonium can be distinguished from ubiquitous nuclear weapons fallout via its characteristic high  $^{240}\text{Pu}/^{239}\text{Pu}$  isotopic

ratio. Fallout plutonium in Japan is characterized by a low  $^{240}\text{Pu}/^{239}\text{Pu}$  ratio in the range of 0.15–0.23.<sup>30</sup> Environmental samples impacted by reactor plutonium from the FDNPP accident have a  $^{240}\text{Pu}/^{239}\text{Pu}$  isotopic ratio of typically >0.30.<sup>8,10,31</sup> The  $^{240}\text{Pu}/^{239}\text{Pu}$  isotopic ratios found in the soil samples analyzed in this study ranged between 0.16 and 0.22 (Table S3 and Figure S4), and hence do not provide evidence for a contamination with reactor Pu. However, since Pu is distributed in particulate form, this negative result could also be caused by a kind of “nugget” effect: If no Pu particle has been present in the very sampling site, this could pretend the lack of environmental reactor Pu, although it may have been present in other spots of the very location.

A strong affirmation for the hypothesis of resuspended radioactive dust comes from  $^{90}\text{Sr}$  analysis. Only three soil samples revealed detectable concentrations of  $^{90}\text{Sr}$ . Two spots had very low activity concentrations: site 8–3 with  $^{90}\text{Sr}$  of  $1.3 \pm 0.1 \text{ Bq kg}^{-1}$ ; site 7–1 with  $^{90}\text{Sr}$  of  $1.9 \pm 0.2 \text{ Bq kg}^{-1}$ . One site (1–2) that is located in the center of the simulated plume, however, exhibited significant  $^{90}\text{Sr}$  activity concentrations of  $78 \pm 8 \text{ Bq kg}^{-1}$ . This is approximately in the same range as previously reported  $^{90}\text{Sr}$  levels in the suspicious vegetation sample from Minamisoma from December 2011 ( $125 \text{ Bq kg}^{-1}$ )—and only 1 order of magnitude lower than what has been found just outside the FDNPP site in 2011.<sup>7</sup> The  $^{90}\text{Sr}/^{137}\text{Cs}$  activity ratio in this study was 0.04, which is a very high ratio. The suspicious Minamisoma vegetation sample from 2011 also had an exceptionally high  $^{90}\text{Sr}/^{137}\text{Cs}$  activity ratio of 0.1. As nuclear weapons fallout has a relatively high  $^{90}\text{Sr}$  component compared with a nuclear accident, pre-Fukushima background of radionuclides in soil had a  $^{90}\text{Sr}/^{137}\text{Cs}$  ratio of up to 1.1, albeit at much lower overall activity levels.<sup>32</sup>

In summary, this study reveals significant intermittent releases of airborne radionuclides in August 2013, long after the initial releases caused by the Fukushima nuclear accident in spring 2011. Increased activities were observed at the air filter station in Haramachi/Minamisoma in the week of August 15 to 22, 2013. Although the resuspension of deposited radionuclides has been identified as a potent source for transport of radioactive contaminants,<sup>24,25</sup> we could show herein that in fact the site of FDNPP is likely to be the source of one of the most pronounced sporadic releases since the accident. Modeling confirms that debris removal actions taking place in this week are likely to have contaminated the area of Minamisoma that has had very low contamination levels previously. Total  $^{137}\text{Cs}$  and plutonium deposition as well as  $^{134}\text{Cs}/^{137}\text{Cs}$  activity ratios and  $^{240}\text{Pu}/^{239}\text{Pu}$  isotopic ratios observed in soil remain inconclusive to support the hypothesis. However, one extraordinary high contamination of soil with  $^{90}\text{Sr}$  in the center of the simulated plume indicates the contamination of the location with dust particle stemming from the FDNPP site. The high non-uniformity of the contamination levels and  $^{134}\text{Cs}/^{137}\text{Cs}$  signatures is most probably due to non-uniform deposition of radioactive particulate matter, causing high local fluctuations in the soil samples taken in the course of this study. Our results indicate that a total of  $2.8 \times 10^{11} \text{ Bq } ^{137}\text{Cs}$  has been released from the FDNPP site by resuspension in the course of the debris removal operations on August 19, 2013. This release corresponds to approximately 1/50 000 of Fukushima’s total atmospheric releases of  $^{137}\text{Cs}$  ( $14.5 \text{ PBq}$ ).<sup>33</sup> Finally, this study evidences that significant secondary releases of radionuclides by resuspension processes and eolian transport



of contaminated particles are conceivable scenarios in the future. Most importantly, the ongoing decommissioning and dismantling activities of the crippled Fukushima reactors, thereby, pose an imminent health threat for future decades. A resuspension of highly contaminated particles from the FDNPP site not only involves the risk of a massive radiocesium dispersion; these particles are likely to carry an even more hazardous load such as less volatile, bone-seeking  $^{90}\text{Sr}$  or actinides (including plutonium).

## ■ ASSOCIATED CONTENT

### Supporting Information

The Supporting Information is available free of charge on the ACS Publications website at DOI: 10.1021/acs.est.5b03155.

Figure S1. Location of Minamisoma City and the soil sampling locations in the area. Figure S2. Cesium-137 deposition (to 15 cm depth) at the sampling sites around Minamisoma. Figure S3. Depth profile of the  $^{134}\text{Cs}/^{137}\text{Cs}$  activity ratios in the soil drill cores. The reference corresponds to the “integral” signature of the Fukushima accident of 0.98 at the time of the accident,<sup>28</sup> decay corrected to the time of sampling (September 7, 2014). Figure S4. Isotopic ratios of  $^{240}\text{Pu}/^{239}\text{Pu}$  in soil samples in the Minamisoma area (PDF)

Table S1. Geographical soil sample information and gamma-spectroscopic results of soil samples from the Minamisoma area. Table S2. Radiocesium ratio in whole airborne sporadic releases in different sites and sampling times (XLSX)

Table S3. Results of plutonium analyses of soil samples from the Minamisoma area (XLSX)

## ■ AUTHOR INFORMATION

### Corresponding Author

\*E-mail: koizumi.akio.5v@kyoto-u.ac.jp. Phone: 81-75-753-4456. Fax: 81-75-753-4458.

### Notes

The authors declare no competing financial interest.

## ■ ACKNOWLEDGMENTS

This work was supported by JSPS KAKENHI (Grant Numbers 26293150 and 25870158), Bousaiken Grant 26P-01, and the U.S. Nuclear Regulatory Commission (NRC) (Grant number NRC-HQ-12-G-38-0044). The authors gratefully acknowledge the NOAA Air Resources Laboratory (ARL) for the provision of the HYSPLIT transport and dispersion model that was used for the Table of Contents graphic.<sup>34</sup>

## ■ REFERENCES

(1) Yasunari, T. J.; Stohl, A.; Hayano, R. S.; Burkhart, J. F.; Eckhardt, S.; Yasunari, T. Cesium-137 deposition and contamination of Japanese soils due to the Fukushima nuclear accident. *Proc. Natl. Acad. Sci. U. S. A.* **2011**, *108* (49), 19530–4.

(2) Harada, K. H.; Niisoe, T.; Imanaka, M.; Takahashi, T.; Amako, K.; Fujii, Y.; Kanameishi, M.; Ohse, K.; Nakai, Y.; Nishikawa, T.; Saito, Y.; Sakamoto, H.; Ueyama, K.; Hisaki, K.; Ohara, E.; Inoue, T.; Yamamoto, K.; Matsuoka, Y.; Ohata, H.; Toshima, K.; Okada, A.; Sato, H.; Kuwamori, T.; Tani, H.; Suzuki, R.; Kashikura, M.; Nezu, M.; Miyachi, Y.; Arai, F.; Kuwamori, M.; Harada, S.; Ohmori, A.; Ishikawa, H.; Koizumi, A. Radiation dose rates now and in the future for residents neighboring restricted areas of the Fukushima Daiichi Nuclear Power Plant. *Proc. Natl. Acad. Sci. U. S. A.* **2014**, *111* (10), E914–E923.

(3) Kinoshita, N.; Sueki, K.; Sasa, K.; Kitagawa, J.-I.; Ikarashi, S.; Nishimura, T.; Wong, Y.-S.; Satou, Y.; Handa, K.; Takahashi, T.; Sato, M.; Yamagata, T. Assessment of individual radionuclide distributions from the Fukushima nuclear accident covering central-east Japan. *Proc. Natl. Acad. Sci. U. S. A.* **2011**, *108* (49), 19526–9.

(4) Steinhauser, G.; Brandl, A.; Johnson, T. E. Comparison of the Chernobyl and Fukushima nuclear accidents: A review of the environmental impacts. *Sci. Total Environ.* **2014**, *470–471*, 800–817.

(5) Lepage, H.; Evrard, O.; Onda, Y.; Lefevre, I.; Laceby, J. P.; Ayrault, S. Depth distribution of cesium-137 in paddy fields across the Fukushima pollution plume in 2013. *J. Environ. Radioact.* **2015**, *147*, 157–164.

(6) Yoshida, N.; Kanda, J. Tracking the Fukushima Radionuclides. *Science* **2012**, *336* (6085), 1115–1116.

(7) Steinhauser, G.; Schauer, V.; Shozugawa, K. Concentration of strontium-90 at selected hot spots in Japan. *PLoS One* **2013**, *8* (3), e57760.

(8) Schneider, S.; Walther, C.; Bister, S.; Schauer, V.; Christl, M.; Synal, H.-A.; Shozugawa, K.; Steinhauser, G. Plutonium release from Fukushima Daiichi fosters the need for more detailed investigations. *Sci. Rep.* **2013**, *3*, 2988.

(9) Schwantes, J. M.; Orton, C. R.; Clark, R. A. Analysis of a nuclear accident: fission and activation product releases from the Fukushima Daiichi nuclear facility as remote indicators of source identification, extent of release, and state of damaged spent nuclear fuel. *Environ. Sci. Technol.* **2012**, *46*, 8621–8627.

(10) Zheng, J.; Tagami, K.; Watanabe, Y.; Uchida, S.; Aono, T.; Ishii, N.; Yoshida, S.; Kubota, Y.; Fuma, S.; Ihara, S. Isotopic evidence of plutonium release into the environment from the Fukushima DNPP accident. *Sci. Rep.* **2012**, *2*, 304.

(11) Steinhauser, G. Fukushima's forgotten radionuclides: A review of the understudied radioactive emissions. *Environ. Sci. Technol.* **2014**, *48*, 4649–4663.

(12) Mahara, Y.; Miyahara, S. Residual plutonium migration in soil of Nagasaki. *J. Geophys. Res.* **1984**, *89* (B9), 7931–7936.

(13) Kocadag, M.; Musilek, A.; Steinhauser, G. On the interference of  $^{210}\text{Pb}$  in the determination of  $^{90}\text{Sr}$  using a strontium specific resin. *Nucl. Technol. Radiat. Prot.* **2013**, *28* (2), 163–168.

(14) Bisinger, T.; Hippler, S.; Michel, R.; Wacker, L.; Synal, H. A. Determination of plutonium from different sources in environmental samples using alpha-spectrometry and AMS. *Nucl. Instrum. Methods Phys. Res., Sect. B* **2010**, *268* (7–8), 1269–1272.

(15) Stocker, M.; Döbeli, M.; Grajcar, M.; Suter, M.; Synal, H.-A.; Wacker, L. A universal and competitive compact AMS facility. *Nucl. Instrum. Methods Phys. Res., Sect. B* **2005**, *240* (1–2), 483–489.

(16) Vockenhuber, C.; Alfimov, V.; Christl, M.; Lachner, J.; Schulze-König, T.; Suter, M.; Synal, H. A. The potential of He stripping in heavy ion AMS. *Nucl. Instrum. Methods Phys. Res., Sect. B* **2013**, *294* (0), 382–386.

(17) Christl, M.; Casacuberta, N.; Lachner, J.; Maxeiner, S.; Vockenhuber, C.; Synal, H.-A.; Goroncy, I.; Herrmann, J.; Daraoui, A.; Walther, C.; Michel, R. Status of  $^{236}\text{U}$  analyses at ETH Zurich and the distribution of  $^{236}\text{U}$  and  $^{129}\text{I}$  in the North Sea in 2009. *Nucl. Instrum. Methods Phys. Res., Sect. B* **2015**, *361*, 510–516.

(18) Dai, X.; Christl, M.; Kramer-Tremblay, S.; Synal, H.-A. Ultra-trace determination of plutonium in urine samples using a compact accelerator mass spectrometry system operating at 300 kV. *J. Anal. At. Spectrom.* **2012**, *27* (1), 126–130.

(19) Christl, M.; Vockenhuber, C.; Kubik, P. W.; Wacker, L.; Lachner, J.; Alfimov, V.; Synal, H. A. The ETH Zurich AMS facilities: Performance parameters and reference materials. *Nucl. Instrum. Methods Phys. Res., Sect. B* **2013**, *294*, 29–38.

(20) Grell, G. A.; Peckham, S. E.; Schmitz, R.; McKeen, S. A.; Frost, G.; Skamarock, W. C.; Eder, B. Fully coupled “online” chemistry within the WRF model. *Atmos. Environ.* **2005**, *39* (37), 6957–6975.

(21) Grell, G. A.; Barth, M.; Freitas, S. R.; Pfister, G.; Carmichael, G.; Fast, J.; McHenry, J.; McQueen, J.; Pleim, J.; Schere, K. L.; Skamarock, W. C.; Schmitz, R.; Westphal, D.; Peckham, S.; Chang, J. *Weather*

Research and Forecasting (WRF) Model; <http://ruc.noaa.gov/wrf/WG11/> (Accessed June 2015).

(22) Saito, K.; Fujita, T.; Yamada, Y.; Ishida, J.-i.; Kumagai, Y.; Aranami, K.; Ohmori, S.; Nagasawa, R.; Kumagai, S.; Muroi, C.; Kato, T.; Eito, H.; Yamazaki, Y. The Operational JMA Nonhydrostatic Mesoscale Model. *Mon. Weather Rev.* **2006**, *134* (4), 1266–1298.

(23) Nuclear Regulation Authority (NRA) Assessment for radionuclide emission involved in the debris removal operation for the reactor 3; Handout for 28th conference for supervision of a specific nuclear facility (in Japanese); [www.nsr.go.jp/data/000051154.pdf](http://www.nsr.go.jp/data/000051154.pdf) (Accessed June 2015).

(24) Hirose, K. Temporal variation of monthly  $^{137}\text{Cs}$  deposition observed in Japan: Effects of the Fukushima Daiichi nuclear power plant accident. *Appl. Radiat. Isot.* **2013**, *81*, 325–329.

(25) Hirose, K. Two-years trend of monthly  $^{137}\text{Cs}$  deposition observed in Kanto and south Tohoku areas, Japan: effects of the Fukushima Dai-ichi nuclear power plant accident. *J. Radioanal. Nucl. Chem.* **2015**, *303*, 1327–1329.

(26) Fukushima Prefecture Monthly radioactive deposition monitoring 2013 (provisional figure) (in Japanese); [http://www.pref.fukushima.lg.jp/sec\\_file/monitoring/etc/gekkankoukabutu25nendo.pdf](http://www.pref.fukushima.lg.jp/sec_file/monitoring/etc/gekkankoukabutu25nendo.pdf) (Accessed June 2015).

(27) Kirchner, G.; Bossew, P.; De Cort, M. Radioactivity from Fukushima Dai-ichi in air over Europe; part 2: what can it tell us about the accident? *J. Environ. Radioact.* **2012**, *114*, 35–40.

(28) Merz, S.; Steinhauser, G.; Hamada, N. Anthropogenic radionuclides in Japanese food: environmental and legal implications. *Environ. Sci. Technol.* **2013**, *47* (3), 1248–1256.

(29) TEPCO Press Conference. In *Analysis of dust filters collected at the sampling site on the roof of Fukushima Daiichi Nuclear Power Plant Reactor Unit 3*, in Japanese; May 12, 2015.

(30) Yang, G.; Zheng, J.; Tagami, K.; Uchida, S. Plutonium concentration and isotopic ratio in soil samples from central-eastern Japan collected around the 1970s. *Sci. Rep.* **2015**, *5*, 9636.

(31) Evrard, O.; Pointurier, F.; Onda, Y.; Chartin, C.; Hubert, A.; Lepage, H.; Pottin, A.-C.; Lefèvre, I.; Bonté, P.; Laceby, J. P.; Ayrault, S. Novel insights into Fukushima nuclear accident from isotopic evidence of plutonium spread along coastal rivers. *Environ. Sci. Technol.* **2014**, *48* (16), 9334–9340.

(32) Igarashi, Y.; Otsuji-Hatori, M.; Hirose, K. Recent deposition of  $^{90}\text{Sr}$  and  $^{137}\text{Cs}$  observed in Tsukuba. *J. Environ. Radioact.* **1996**, *31* (2), 157–169.

(33) Katata, G.; Chino, M.; Kobayashi, T.; Terada, H.; Ota, M.; Nagai, H.; Kajino, M.; Draxler, R.; Hort, M. C.; Malo, A.; Torii, T.; Sanada, Y. Detailed source term estimation of the atmospheric release for the Fukushima Daiichi Nuclear Power Station accident by coupling simulations of an atmospheric dispersion model with an improved deposition scheme and oceanic dispersion model. *Atmos. Chem. Phys.* **2015**, *15* (2), 1029–1070.

(34) Draxler, R. R.; Rolph, G. D. HYSPLIT (HYbrid Single-Particle Lagrangian Integrated Trajectory) Model access via NOAA ARL READY Website; <http://ready.arl.noaa.gov/HYSPLIT.php> (Accessed June 2015).